QTL Mapping of Fruit and Seed-related Traits in Watermelon Using Genotyping-by-Sequencing-based High-density Linkage Mapping

Meiling Gao (gaomeiling0539@163.com)
College of Life Sciences, Agriculture and Forestry, Qiqihar University, Qiqihar https://orcid.org/0000-0002-0150-2999

Xiaoxue Liang
Qiqihar University

Xiujie Liu
Qiqihar Horticulture Research Institute

Yu Guo
Qiqihar University

Hongguo Xu
Qiqihar University

Jixiu Liu
Qiqihar Horticultural Research Institute

Yue Gao
Qiqihar Horticultural Research Institute

Chengzhi Yuan
Qiqihar University

Feishi Luan
Northeast Agricultural University

Research article

Keywords: Watermelon, QTL mapping, Fruit quality, Fruit Size, Genotyping-by-Sequencing

Posted Date: November 24th, 2020

DOI: https://doi.org/10.21203/rs.3.rs-107825/v1

Abstract

Background

Watermelon is an important vegetable crop with dual use of both fruit and seeds. Understanding the genetic basis of fruit quality and seed size-related traits is important for efficient marker-assisted breeding in watermelon. Linkage mapping in watermelon segregating populations using genotyping-by-sequencing (GBS) provides insights into genetic control of fruit- and seed-related traits and genome collinearity in commercial watermelon cultivars.

Results

In the present study, we conducted QTL mapping of 12 horticulturally important traits on external and internal fruit quality and seed size/weight using segregating populations derived a cross between two commercial varieties. A high-density genetic map was developed with GBS which contained more than 6,000 SNP loci in 1,004 bins with a total map length of 1261.1 cM and average marker interval of 1.26 cM or 329 kb. Phenotypic data of fruit rind color (RC), rind stripe pattern (RSP), flesh color (FFC), fruit diameter (FD), fruit length (FL), fruit shape index (FSI), fruit weight (FW), Brix content central (BCC), Brix content edge (BCE), seed length (SL), width (SW), and weight (20SWT) were collected from two locations in two years. QTL analysis identified 47 QTL for the 12 traits, of which 24 had moderate- or major-effects, and 34 were novel QTL not identified in previous studies. The QTL for RSP were identified overlapped with previous reports, and mapped the QTL to a small interval on chromosome 6. From the detected novel QTL, we identify FD (*qfd2.1*), FL (*qfl2.1*) co-located with FSI (*qfsi2.1*) QTL on chromosome 2, and the minor QTL *qfw3.2* co-located with previously reported fruit shape QTL (*qfd3.1*, *qfl3.1*, *qfsi3.1*), and SW (*qsw10.1*) co-located with 20SWT QTL (*q20swt10.1*) on chromosome 10, and 5 minor QTL (*qbcc2.1*, *qbcc5.1*, *qbce2.1*, *qbce2.2*, *qbce5.1*) were found to be likely new locus for Brix content.

Conclusion

We conducted GBS consisting of 120 F_2 individuals and developed a high-density linkage map with more than 6,000 SNP loci in 1004 bins in watermelon. We identified 47 QTL for 12 fruit and seed related traits including 34 novel QTL. Our work expands the molecular breeding toolbox for watermelon to improve the yield and fruit quality.

Background

Watermelon (*Citrullus lanatus*, $2n = 2x = 22$, family Cucurbitaceae) is a popular vegetable fruit crop. Watermelon was originated in Africa, and now is growing worldwide [1]. New watermelon varieties with enhanced fruit quality are needed to meet the increasing demands from consumers. Recent progress in the development of genome assemblies and high-density genetic maps, and the use of of high-throughput genotyping methods are accelerating QTL mapping and cloning studies in watermelon. For example, genotyping-by-sequencing (GBS) [2] is being widely used in many crop plant for various marker-

based studies [3–6]. In watermelon, GBS has recently been used to characterize collections of accessions [7–9] and biparental populations [10–13].

Watermelon breeding traditionally focused on seed, fruit quality and morphological characteristics [14]. Due to the increasing availability of genetic and genomics resources in watermelon [15], significant progress has been made in understanding the genetic basis of horticulturally important traits and development of molecular markers [7–10, 13, 15–19]. For example, watermelon fruit rind color (RC) is important since the appearance is one of the main determinants for consumer preference in the market, which could be dark green or light green, light green-gray or yellow [14, 20–21]. Several studies investigated the inheritance of watermelon RC, and identified molecular markers and candidate genes for RC. For example, the yellow skin phenotype in watermelon was found to be controlled by genes on chromosome 4 including the same locus of *Dgo* [22], *yellow skin* [23], *Clyr* [24]. The green skin was proposed to be controlled by genes on chromosome 8 by the *D* [22], or *qrc-c8-1* [13] loci, and *ClCGMenG* has been identified as candidate gene for *D/rc-c81* [25].

Watermelon rind stripe pattern (RSP) is another important appearance trait affecting buying habits of consumers. Several studies investigated the inheritance of RSP [20, 26–30]. They include irregularly distributed and randomly shaped whitish to green spots (*m*), pencilled lines on skin (*p*), spotted fruit rind (*Sp*), yellow belly (*Yb*), stripe pattern (*S*), intermittent stripes (*ins*), blurred stripe margin (*Csm*), wide stripe (g^W), medium stripe (g^M), narrow stripe (g^N). Genes responsible for RSP have been identified on chromosome 6 including locus of *AT14-900* [31–32] associated with clearly defined stripes/blurred stripes, *S* [9, 19, 22] associated with stripe pattern/non-stripe pattern. A major-effect QTL *RS8.1* for the rind stripe width was located on chromosome 8 [33]. The chromosomal location of the *S* is unknown.

There are different colors of watermelon flesh that are visually appealing. The main flesh colors for watermelon are white (*Wf*), pale yellow (*py*), canary yellow (*C*), orange (y^o), pink (*c*), and red (*Y*), some *C. amarus* accessions have light green flesh color [20, 34–36]. Several studies in both bi-parental and natural populations have identified the *lycopene β-cyclase* gene (*LCYB*, *Cla97C04G070940*) on watermelon chromosome 4 that is responsible for the red flesh color [19, 35–38]. These studies indicated that the mutation in *LCYB*, which possibly leads to increased lycopene accumulation, results in the red flesh color in most cultivars [39–41]. Other studies suggest that the regulation of expression of the *PSY* gene for phytoene synthase may contribute to the transition from pale-colored to red, orange or yellow flesh by increasing total carotenoid production [12, 42]. Limited work has been done on molecular mapping of other flesh colors in watermelon.

The content of soluble sugars is a major fruit quality trait of watermelon, which was under strong selection during domestication and breeding[42]. Fruit sugar accumulation seems to be regulated by quantitative trait loci [43]. In QTL mapping using segregating populations derived from the crosses between a sweet-dessert watermelon line and the unsweet accessions, a major-effect QTL for Brix value, *QBRX2*-1 was identified [15, 17]. 96 recombinant inbred lines derived from crossing sweet with unsweet

varieties were resequenced, and a candidate gene (*Cla00264*) for the previously identified *QBRX2-1* [15, 17] on chromosome 2 was identified, which is a *C. lanatus tonoplast sugar transporter 2* (*ClTST2*) [43].

Fruit and seed sizes are also important target traits in watermelon breeding. The fruit shape of watermelon may be round, oval, or elongated. A single gene (*O/o*) with incomplete dominance was proposed to determine the difference between elongated and round fruits: *OO*, for elongated, *Oo*, for blocky, and *oo* for round fruits, respectively [26, 45–46]. However, many later studies have suggested the quantitative nature of fruit size and shape in watermelons [47–49]. After review of the literature, Pan et al. (2020) suggested 15, 9, and 6 consensus QTL for watermelon fruit size, shape and weight, respectively [50]. The seed size of watermelon varieties vary greatly which were classified into six groups: giant, big, medium, small, tiny, and tomato seed [51]. Guo et al. (2020) reviewed the seed QTL in watermelon and inferred 14 consensus QTL [1, 17, 52–55]. It should be noted that the QTL mapping studies on watermelon seed size/weight are very limited. The genomic regions harboring these QTL are still very large.

In watermelon, most QTL mapping studies for various horticultural traits used segregating populations from crosses between exotic (wild) accessions and cultivated inbred lines. The inheritance of those traits in populations derived from crosses among elite watermelon varieties has not been evaluated. The objective of this study was to identify QTL underlying 12 fruit and seed-related traits in segregating populations developed from two elite watermelon cultivars. Using GBS, we developed a high density linkage map with more than 6000 SNP loci. Phenotypic data for 12 traits were collected in F_2 and F_3 populations from multi-year trials. Novel QTL were detected for a number of those traits.

Methods

Plant materials

The two parental lines used in this study included K2 and L1 that are different in multiple fruit and seed related traits. K2 is a Chinese variety setting oval shaped fruit with dark green, smooth rind and red flesh. L1 is a Japanese variety bearing round fruit with light green but striped rinds and yellow flesh (Fig. 1). Seeds of L1 are slightly larger than those of K2. Both inbred lines have medium size fruits and high soluble solid contents that are widely accepted in Asian markets. Seeds of both lines were kindly provided by the Qiqihar Horticultural Research Institute, Qiqihar, China.

An F_2 population of 120 plants from K2 × L1 mating was used for developing a linkage map and initial QTL mapping. Phenotypic data collection and validation of detected QTL in target chromosomal regions were also conducted with 120 $F_{2:3}$ families of the same population.

Phenotypic data collection of fruit and seed-related traits

Phenotypic data collection for the F_2 and $F_{2:3}$ populations were conducted in the greenhouses in summer 2016 (Experiment 2016F2) and in the open field in summer 2017 (Experiment 2017F3) of the Qiqihar Horticultural Research Institute (Qiqihar, Heilongjiang Province, China, 47°42´N, E123°99´), respectively. The details of each experiment are provided in Supplemental Table S1. Data for 10 and 5 traits were collected in F_2 and $F_{2:3}$ populations (total 12), respectively. Fruit and seed traits were measured on mature fruits (>35 days after pollination). For F_2, the data were collected from individual plants. For each F_3 family, at least 8 plants were used for data collection (1 fruit per plant), and the family means were used in QTL analysis.

Upon harvest, the fruits were first visually scored for rind stripe pattern (RSP), and rind color (RC), then cut open longitudinally to score for flesh color (FFC). The RC of each fruit was scored categorically as light green, dark green, or a mixture of dark green and light green, which was assigned a numerical value of 3, 1, and 2, respectively. RSP was scored as 1 for non-striped, 3 for striped, and 2 for the mixture of striped and non-striped. Similarly, FFC of a fruit could be scored for 3 (yellow), 1 (red), or 2 (a mixture of the two). Fruit weight (FW) was measured on a per fruit basis. Fruit shape index (FSI) was the ratio of FL (fruit length from stem end to flower end) to FD (equatorial fruit diameter). The degree of Brix (BRX) was measured using a refractometer (Atago Co., Ltd., Tokyo, Japan) from a juice sample collected from the center (BCC) or the edge (BCE) of the fruit following Sandlin et al. (2012) [15]. Seeds were extracted from each harvested fruit. The seed weight of each fruit was the mean from three replications of 20 fully developed seeds (20SWT). Seed length (SL) and seed width (SW) were measured using a Vernier caliper based on 20 randomly selected seeds per fruit. For each trait, the value of each F_2 plant, or family mean of each $F_{2:3}$ family were used in QTL analysis.

Statistical analyses and graphical presentations of phenotypic data were performed using R (v3.2.3) with the R Studio v1.0.143 interface. To obtain the correlation matrix among traits, the Pearson correlation coefficients were calculated with the R package “Hmisc” [56].

Genotyping by sequencing and linkage map construction

Young leaves from individual F_2 plants and parental lines were collected from 2016F2 trial for genomic DNA extraction following established protocols [57]. Genotyping by sequencing (GBS) for the 120 F_2 plants was performed on an Illumina Hi-Seq 4000 (Illumina, San Diego, CA) through commercial service by Guangzhou Genedenovo Biotechnology Co., Ltd (http://www.genedenovo.com/) following manufacturer’s protocols. The two parental lines, K2 and L1, were re-sequenced with Illumina Hi-Seq 2500 to ~20× coverage. The raw reads were sorted according to indices, and the high-quality SNPs between parents were called by alignment against the 97103 watermelon draft genome 97103 (V1.0) [58] (available at http://www.cucurbitgenomics.org/) using the Burrows-Wheeler Aligner (BWA) [59] and VarScan2 [60].

For GBS data from the 120 F_2 plants, variant calling was performed using 97103 V1.0 as the reference with the GATK's Unified Genotyper, and the resulting SNPs/Indels were filtered using GATK's Variant Filtration [61]. ANNOVAR [62] was used to annotate SNPs or InDels. The following criteria were used to filter for high quality SNP for linkage map development: (1) homozygous in F_2 individuals and are congruent with parental lines; (2) reads depth coverage >4× in parental lines; 3) biallelic with aa×bb segregation pattern. SNPs showing distorted segregation were also excluded. The final set of SNPs was used to define a bin in which all SNPs are co-segregating (no recombination) in the 120 F_2 plants. A single variant with the lowest number of missing data was selected to represent each bin, and only bins with <30% missing data were kept for bin map construction.

The linkage map was constructed using JoinMap V4.1. Based on sequences associated with the markers, each linkage group was assigned to a chromosome. The markers were ordered based on maximum likelihood (ML), and the genetic distance between markers was calculated with the Kosambi mapping function. Haplotypes and heatmaps were constructed using the "draw haplotype-map.pl" and "draw heatmap.pl" perl scripts, respectively. Collinearity between genetic and physical positions of mapped loci was determined by plotting genetic marker positions (in cM) against their physical positions (in Mbp), which was confirmed by BLAST searches. In addition, Spearman's correlation coefficients were calculated to assess the collinearity between the genetic and physical maps.

QTL analysis

QTL analysis was performed with R/qtl (http://www.rqtl.org/) [63]. Genomewide identification of QTL was performed with the composite interval mapping (CIM) method following Weng et al. (2015) [64]. LOD threshold ($P < 0.05$) for declaring significant QTL was determined using 1,000 permutations [65-66]. For each detected QTL, a 1.5-LOD support interval was calculated to define the left and right markers.

Naming of QTL followed recommendations by Bo et al. (2015) [67], and Pan et al. (2020) [50]. For example, *qfd2.1* and *qfsi3.1* designated the first QTL for fruit diameter and fruit shape index in watermelon chromosomes 2 and 3, respectively.

Results

Phenotypic analysis of fruit and seed related traits

In 2016F2, we collected phenotypic data for 10 traits (RC, RSP, FFC, FW, FD, FL, FSI, 20SWT, SL and SW). In 2017F3 experiment, data for FW, FD, FL, FSI, BCC, BCE, RSP, RC, and FFC were collected for QTL validation (Supplemental Table S1) (BCC and BCE were not recorded in 2016F2). Typical fruits for the two parental lines, their F_1, and F_2 plants are shown in Fig. 1. The segregation ratio of RC, RSP and FFC among the F_2 population is presented in Table 1. The phenotypic means, standard deviation and range of these traits in both experiments are presented in Table 2.

To evaluate the mode of inheritance of RC, RSP and FFC in watermelon fruit, parents and F_1 were grown in parallel, evaluated for rind color, rind stripe pattern and flesh color. The data regarding RC, RSP and FFC were collected by visual analysis. The rind colors (RC) of the fruits of K2 and L1 were dark green and light green, respectively. The F_1 hybrid was intermediate between the parental hues. In the F_2 generation, three categories of rind colors could be recognized: dark green, light green, and irregular color patterns consisting of mixed dark green and light green. In 2016F2 experiment, the F_2 population separated into 83 plants with dark green rind (include plants that exhibit color consistent with F_1) and 37 plants with light green rind which was in agreement with a 3:1 ratio (χ^2=2.178, *P*=0.14). Based on the segregation among the 120 $F_{2:3}$ families, 21, 37, and 62 were homozygous dark green, homozygous light green, heterozygous at the rind color locus. These data further support a major-effect QTL underlying rind color segregation in this population.

The rind stripe patterns (RSP) of the fruits of K2 and L1 are non-striped and striped, respectively. The F_1 had rind stripe pattern but differs from L1 (Fig. 1). In the 2016F2 experiment, among the 120 F_2 individuals, 92 (include individuals that exhibit striped consistent with F_1) and 28 were striped and non-striped, respectively which was consistent with the 3 to 1 segregation ratio (Table 1). Segregation in 120 $F_{2:3}$ families revealed that 28 were homozygous non-striped, 37 were homozygous striped, and 55 were heterozygous at the rind stripe pattern locus.

The flesh color (FFC) of K2 and L1 fruits were red and pale yellow, respectively, while that of their F_1 was yellow or pale yellow (Fig. 1) suggesting dominance of the pale yellow flesh color over red. yellow (including mixed yellow and red color)there were 28 $F_{2:3}$ families with red flesh color, 66 with mixed colors, and 26 with yellow (Table 2). Thus, all the segregation results suggested that rind color, rind stripe pattern and flesh color are largely simply inherited in this population. Nevertheless, additional QTL may exist for each which could be evidenced from QTL mapping results (see below).

Fruit size/shape (FL, FD, and FSI) and weight (FW) data were collected in both F_2 and $F_{2:3}$ populations in two years. The frequency distributions of the four traits in the two populations are illustrated in Fig. 2. In both experiments, all four traits showed a largely normal distribution suggesting their quantitative nature. But for FW, FL and FD, the population in 2017F3 shifted toward larger and heavier fruits which may be due partially to differences in culture practices (Fig. 2; Table 2). In the 2017F3 experiment, plastic mulch was used which may increase soil temperature, accelerate flowering and fruit growth. Interestingly, while FL of F_1 was close to the mid-parental value, FW and FD was much larger than either parent suggesting heterosis for them in this population. This may also suggest that FD contributes significantly to FW. In addition, despite the different distributions of FL and FD between F_2 and $F_{2:3}$ populations, the frequency distributions of FSI in the two experiments were highly consistent suggesting FSI is a more stable indicator for fruit growth. Finally, for all the four traits in both experiments, transgressive inheritance was obvious suggesting different genetic basis of these four traits in the two parental lines.

Data for three seed traits (20SWT, SL and SW), and two Brix-related traits (BCC and BCE) were collected in a single experiment. The frequency distribution for the five traits is presented in Supplemental Fig. S1. All showed largely normal distribution suggesting their quantitative inheritance nature.

We examined correlations among these traits, and the Pearson's correlation coefficient matrix among these traits is presented in Supplemental Fig. S2. As expected, correlations between fruit dimensions (FL and FD) and FW are strong and positive. The correlation between FSI and FL was higher than with FD, implying that length is the major determinant of fruit shape in this population, which could be seen from closely linked QTL for these traits (below). The correlation between FD and FW was higher than that of FL, which may be related to the transgressive inheritance of FD and FW. There was also a high correlation between the BCC and BCE. Positive correlations among 20-SWT, SL and SW were significant and strong.

GBS data analysis and linkage map construction

Using Illumina high throughput sequencing, we sequenced the two watermelon elite inbred lines K2 and L1. After SNP filtering, 76,970,496 and 68,785,644 high quality resequencing reads were mapped to the 97103 V1.0 watermelon reference genome for K2 and L1, representing 10,926, and 9,764 Mbp sequences, respectively (see Supplemental Table S2 for main statistics). Thus the depth of coverage for K2 and L1 was approximately 25.7× and 22.9×, respectively. In total, 365,148 SNPs and 75,111 indels were identified between K2 and L1.

Resequencing of 120 F_2 plants resulted in 561,537,056 high quality reads (79,738 Mbp) representing ~1.56× coverage per plant (Table S2). After application of various filtering criteria, there were 13,762 high-quality SNPs that were segregating in the 120 F_2 plants, of which 6,164 followed *aa×bb* segregation pattern, and were used in linkage analysis. Based on recombination events in the 120 F_2 individuals, 1,004 recombinant bins were used to construct the genetic map. Main statistics of the bin genetic map are summarized in Table 3, and graphically presented in Fig. 3. Details of the genetic map and marker locations in the 97103 V1.0 draft genome assembly are presented in Supplemental Table S3. The total length of the genetic map was 1261.1 cM in 11 linkage groups (chromosomes) with Chr2 being the longest (197.1 cM, 146 mapped loci), and Chr10 the shortest (66.7 cM, 60 mapped loci). The main marker interval was 1.26 cM. Physically, the map covered 90.29% of the watermelon genome, with on average 329 kb per bin (Table 3).

Alignment of mapped SNP loci along the physical length (97103 v1.0) of each chromosome is graphically present in Supplemental Fig. S3 indicating uneven distribution of genetic recombination along each chromosome. The genetic map and the watermelon reference genome was highly collinear suggesting correct marker orders on the genetic map, which also implied no large structural changes between the two parental lines that belong to two different market groups. There were still a few large gaps (>2 Mbp) on the genetic map (total 29, Table S2). Nevertheless, overall, the linkage map developed with GBS data and a moderate size segregation population (n=120 F_2) in the present study was of high

quality and very well suited for QTL analysis in the present study and many other applications in the future.

QTL for fruit and seed-related traits in watermelon

The values for 12 traits from F_2 single plant or F_3 family means were employed in QTL analysis. Permutation tests indicated that the LOD thresholds to declare significant QTL among these traits varied from 2.49 to 2.68. For convenience, we used LOD value of 2.5 for all traits. A global view of all QTL detected across the 11 chromosomes is provided in Supplemental Fig. S4. More detailed chromosome views of QTL for all traits are shown in supplemental Fig. S5 (detected in both experiments) and Fig. S6 (detected in only one experiment), respectively. Details of each detected QTL including map location, LOD support value, % of phenotypic variance explained (PVE), additive/ dominance effects, as well as 1.5-LOD support interval are provided in Table 4. Their chromosomal locations are visually illustrated in Fig. 3. Each QTL was assigned a name; if multiple QTL for the same trait detected by different populations (F_2 and F_3) or experiments (2016F2 and 2017F3) were located at the same or nearby locations, the same name was assigned. In total, 47 QTL were detected for the 12 traits including 2 each for RC, 20-SWT, and BCC, 3 each for FSI, SW and BCE, 4 for SL, 5 each for FW and FFC, 6 each for RSP, FL and FD (Table 4).

QTL of rind color (RC) and rind stripe pattern (RSP)

The phenotypic variation of RC and RSP traits was evaluated in two environments (2016F2 and 2017F3). Two QTL, *qrc6.1* and *qrc8.1* were detected for RC. The major-effect QTL *qrc8.1* (PVE = 11.5-15.5%), was identified in both 2016F2 and 2017F3 experiments (Table 4; Fig. S5). The minor-effect QTL *qrc6.1* (PVE = 11.1%) was only detected in 2016F2. The allele from K2 of *qrc8.1* contributed to intensifying RC, while that of *qrc6.1* contributed to weakening RC. Six QTL for RSP, *qrsp1.1*, *qrsp1.2*, *qrsp2.1*, *qrsp2.2*, *qrsp6.1* and *qrsp6.2* were detected from the two experiments (Table 4; Fig. S5). The two minor-effect QTL *qrsp1.1* (PVE = 4.6%) and *qrsp1.2* (PVE = 3.6%) were only detected in 2016F2 and 2017F3, respectively. The three moderate-effect QTL, *qrsp2.1* (PVE = 7.6%), *qrsp2.2* (PVE = 8.0 %), and *qrsp6.1* (PVE = 7.2%) were only detected in one environment. The major effect QTL, *qrsp6.2* (PVE = 33.5-37.7%) was detected in both. The K2 alleles of *qrsp1.1* and *qrsp6.1* reduced RSP (negative additive effects) while all others promoted fruit rind stripe.

QTL of fruit flesh color (FFC)

Five QTL on three chromosomes were identified for fruit flesh color (Table 4; Fig. S5). The QTL *qffc4.1* was detected in both experiments; *qffc2.1* and *qffc5.2* were detected only in 2016F2, whereas *qffc4.2* and *qffc5.1* were identified only in 2017F3. The three minor-effect QTL, *qffc4.2*, *qffc5.1*, and *qffc5.2* could explain 3.9-4.1% observed phenotypic variance; the moderate-effect QTL, *qffc2.1* could explain 10.4% phenotypic variations, and the major effect QTL, *qffc4.1*could explain 10.1-47.3% phenotypic variance. All

QTL had positive additive effects on fruit flesh color. While *qffc5.2* had positive dominance effect, the rest had negative dominance effect.

QTL of fruit BRIX (BCC, BCE)

The data of Brix content were collected from only one season, from which five QTL were detected (Table 4; Fig. S6). The two QTL for BCC, *qbcc2.1* and *qbcc5.1* had LOD support scores of 2.82 (PVE = 12.0%) and 3.33 (PVE = 12.1%), respectively. Three BCE QTL detected in 2017F3 included *qbce2.1* (PVE = 12.6%), *qbce2.2* (PVE = 9.2%), and *qbce5.1* (PVE = 7.5%). The 3 Chr2, and 2 Chr5 QTL had positive, and negative additive effects on Brix, respectively. The two QTL, *qbcc5.1*, and *qbce5.1* were located in the same LOD interval, which may belong to the same locus. This can explain the significant positive correlation between BCC and BCE (Supplemental Fig. S2).

QTL of fruit size and shape (FD, FL, FSI, FW)

Thirteen QTL were detected for FL and FD in two experiments (Table 4; Fig. 4). Among the 6 FD QTL (*qfd2.1*, *qfd2.2*, *qfd3.1*, *qfd6.1*, *qfd8.1* and *qfd9.1*), *qfd2.2* (PVE = 15.5%), and *qfd3.1* (PVE = 15.0%) detected in 2016F2 had the largest effects. However, both were not detected in 2017F3 experiment. The minor-effect QTL *qfd2.1* and *qfd6.1* were only detected in 2016F2 and explained 7.7% and 6.5% of phenotypic variance, respectively. The other two QTL, *qfd8.1* (PVE = 7.2%) and *qfd9.1* (PVE = 11.2%) were only detected in 2017F3. The major-effect QTL *qfd3.1* and the minor-effect QTL *qfd6.1* had negative additive effects on fruit diameter, while the other QTL had positive additive effects on fruit diameter. The opposite effects of different QTL may explain the transgressive inheritance in F_1 (Table 4). Among the 7 FL QTL, *qfl6.1* (PVE = 13.2%) and *qfl8.1* (PVE = 15.2%) were only detected in 2016F2 and 2017F3, respectively. The two minor-effect QTL *qfl2.1* (PVE = 7.2-9.6%) and *qfl5.1* (PVE = 5.5-7.0%) were detected in both years. The major-effect QTL *qfl3.1* (PVE = 19.7%) was only detected in 2016F2 with additive effects on fruit elongation.

There was a significant correlation between FL and FD (Fig. S2), which could be explained by the co-localization of FD and FL QTL on chromosomes 2, 3 and 6 (Table 4). We identified three QTL for FSI in two experiments; the minor-effect QTL *qfsi2.1* and *qfsi2.2* were detected in 2017F3 and 2016F2, respectively, and explained 9.8% and 4.2% of phenotypic variance, respectively; *qfsi3.1* (PVE = 67.6%) was the major-effect QTL and detected in 2016F2, which contributed to increased FSI value (positive additive effects). The locations of all the three FSI QTL were consistent with those of either FL or, FD or both.

Among the 5 FW QTL detected in the two environments, the major-effect QTL *qfw6.1* (PVE = 15.1%) and *qfw8.1* (PVE = 14.0%) were detected in 2016F2 and 2017F3, respectively. The three minor-effect QTL, *qfw2.1*, *qfw3.1*, and *qfw3.2* could explain 8.6-9.4% phenotypic variance. The major-effect QTL *qfw8.1* and the minor-effect QTL *qfw2.1* had positive additive effects on fruit weight, while the other QTL had

negative additive effects on fruit weight. The opposite effects of different QTL may explain the transgressive in heritance in F_1 (Table 4). All five FW QTL seemed to be co-localized with QTL for FL and/or FD (Fig. S5), which was consistent with the significant positive correlation between FW and FL or FD (Supplemental Fig. S2). Thus, FW variation is likely the result of pleiotropic effect of fruit size.

QTL of seed size and weight (SL, SD, 20-SWT)

Although the mean values for the two parental lines were similar, we detected four significant QTL for SL, three for SW, and two for 20SWT in the 2016F2 experiment (Table 4; Fig. S6). Based on chromosomal locations, *qsw2.1*, *qswl2.1*, and *q20swt2.1* seemed to belong to the same locus underlying seed size/weight. The three QTL was the most significant for SW, SL and 20SWT, respectively. The QTL *qsw2.1* was located on chromosomes 2 between markers BIN0194 and BIN0196 with 164.76-167.71 cM intervals, and explained 35.5% of PVE, with a high LOD value of 15.14. The QTL *qsl2.1* (PVE = 43.5%) was located between BIN0192 and BIN0196 (from 163.08 cM to 167.71 cM) with a high LOD value (16.95). The QTL *q20swt2.1* had a LOD score of 21.88, explaining 50.1% of the observed phenotypic variance in this population. These three SL, SW, and 20SWT QTL on chromosome 2 were likely the same major-effect QTL for seed size/weight. Two minor-effect QTL for SW, *qsw3.1* and *qsw10.1*, together explained 18.2% of the PVE values. Three minor-effect QTL for SL *qsl5.1*, *qsl5.2* and *qsl7.1* together explained 16.7% of PVE. The minor-effect QTL for 20SWT, *q20swt10.1* explained 9.0% of the PVE values.

Discussion

A linkage map based on the cross of two elite commercial varieties

In the present study, we developed a high-density genetic map using an F_2 population derived from two elite watermelon varieties K2 and L1, which are popular in the China and Japan markets. Cultivated watermelons are known to have narrow genetic base, and low marker polymorphism is a constraint for genetic map development in pre-genomics era [68-70]. The map developed in the present study had 1004 bins that spanned 1261.1 cM with an average bin interval of 326 kb (Table 3, Table S4). The # of mapped loci (bins) from our study was somewhat lower than maps developed in several previous studies [10,13]. This was reasonable because the two previous maps were developed using populations derived from crosses between wild and cultivated-type watermelons. Several previous studies reported the chromosome rearrangements between the wild and cultivated-type watermelons on chromosomes 1 and 11 [7,8,10,13], which could be due to incorrect assembly of the reference genome, genetic rearrangement or assembly errors [71]. The marker orders of these mapped loci were consistent with their physical locations on the 97103 v1.0 draft genome assembly (Fig. S3) suggesting no major structural changes between K2 and L1 genomes.

Genetic basis of fruit rind color and stripe pattern in watermelon

Fruit rind color and strip patterns are important fruit external quality traits for watermelon. Most watermelon varieties have green or dark green colors (or grey) with or narrow or wide stipes. Several previous studies have shown that watermelon rind color is controlled by a single gene on Chr8 with dark green being dominant to light green [13,22,29]. More recently, Li et al. (2019) identified a candidate gene (*ClCG08G017810* or *ClCGMenG*) for this locus that encodes 2-phytyl-1,4-beta-naphthoquinone methyltransferase [25]. In our study, we consistently detected a major-effect QTL, *qrc8.1* on Chr8 (PVE ~15%) in both years (Table 4; Fig. S5). In the 97103 v1.0 assembly, chromosome 8 is not intact and contains a nearly 262 kb deletion on this chromosome, comprising 34 additional genes at this chromosomal region in 'Charleston Gray'. *ClCGMenG* was from 29869645 to 29901009 on chromosome 8 according to the 'Charleston Gray' watermelon reference genome. However, the 1.5-LOD interval of *qrc8.1* was from 24,074,857 to 24,644,537 (Table 4). Thus our QTL detected in this study seem not in the same region as reported by Li et al. (2019) [25]. Further evidence is needed to prove this. In addition, in 2016F2, we identified a moderate-effect QTL *qrc6.1* that could explain 11.1% observed phenotypic variance (Table 4). Therefore, the gene associated with watermelon rind color in this study merits further investigation.

The rind stripe of watermelon fruit was previously described as a monogenic trait named *S* [26], but to our knowledge it has not been cloned. In this study, we detected six QTL for rind stripe pattern, which explained 3.57-37.65% of the phenotypic variance. A major-effect QTL on this trait, *qrsp6.2* was delimited to a region of 887 kb on chromosome 6 (Table 4; Fig. S5), which was consistent with previous studies in which watermelon rind stripe is controlled by the *S* locus on chromosome 6 [9,19,22]. However, further experiments are necessary to demonstrate the identity of *qrsp6.2*.

QTL for fruit flesh color and fruit Brix in watermelon

Flesh color is probably the most visually appealing trait for watermelon. A major-effect QTL was identified in the F_2 population which was located in an interval of ~ 645 kb. We also identified three minor-effect QTL (*qffc4.2*, *qffc5.1*, *qffc5.2*) and one moderate-effect QTL (*qffc2.1*) for flesh color in this study (Table 4; Fig. S5). Previous studies have shown that flesh color is controlled by several genes, so the appearance of mixed colors may be due to the re-combination of genes controlling the expression of different pigments [35]. The major-effect QTL detected herein seems to be consistent with early work, which suggest that the *LCYB* (*Cla97C04G070940*) gene [19,35-38] leads to increased lycopene accumulation, resulting in the red flesh color in most cultivars [39-41]. Therefore, the new QTL and the new gene associated with watermelon flesh color will require further investigation.

Watermelon fruit is mainly consumed as a dessert; high sugar content and thus high soluble solids is a desired characteristic with special importance in watermelon breeding. Interestingly, of the two elite

parental lines we used in this study, the soluble solid content of K2 was only slightly higher than L1 (Table 2). We detected five soluble solid content QTL, two for BCC (*qbcc2.1*, *qbcc5.1*) and three for BCE (*qbce2.1*, *qbce2.2*, *qbce5.1*) (Table 4; Fig. S6). Based on their LOD intervals, *qbcc2.1*, *qbce2.1* and *qbce2.2* were not co-localized whereas *qbcc5.1* and *qbce5.1* were located in the same interval on Chr5 hinting they may be the same locus for soluble solid content. In previous work, a major QTL for Brix value, *QBRX2-1* was identified on chromosome 2 between nucleotides 17,657,266 and 18,454,759 [15,17,43]. The QTL detected in the present study was located in an interval outside the *ClTST2* (*Cla000264*)the candidate gene for Brix value [43]. Therefore, the gene associated with watermelon sugar accumulation in this study will provide novel QTL and require further investigation.

QTL for fruit size and shape in watermelon

Several QTL mapping studies have been conducted in watermelon to understand the genetic basis of fruit shape variation [1,15,30,54,74]. Pan et al. (2020) reviewed fruit size and shape QTL in the watermelon, from which consensus QTL were inferred including 9 'consensus' FSI QTL on 7 chromosomes (2, 3, 5, 7, 8, 9 and 10) [50]. Among them, the major-effect FSI QTL on chromosome 3, *ClFSI3.1*, has been detected in all QTL mapping studies in watermelon, which is the *O* locus of watermelon proposed long time ago [14,26,50]. Dou et al. (2018) identified a candidate gene for the *O/ClFSI3.1* locus which is a homolog of the tomato *SUN* [1] gene (*ClSun25-26-27a* or *Cla011257*) [74]. Dou et al. (2018) found that the round fruit shape is due to a 159-bp deletion in the coding region of *Cla011257* [74]. This finding was confirmed by Maragal et al. (2019) and Legendre et al. (2020) who reported also a novel allele at this locus [75-76].

In this study, we identified 20 QTL for FL, FD, FSI and FW (Table 4). Among them, *qfsi3.1* had the highest effect (LOD = 32.0; PVE = 67.6%). Other three major-effect QTL, *qfw3.2*, *qfd3.1*, and *qfl3.1* were co-localized with *qfsi3.1* suggesting a single QTL at this locus is responsible for all four traits, and this QTL plays the most important role in control of fruit shape in this population. Based on the chromosomal location, *qfsi3.1* is likely the same as the O/ *ClSun25-26-27a* suggesting that the round fruit shape in majority of cultivated watermelon varieties is controlled by the *O* locus.

Fruit weight (FW) is apparently correlated with fruit size, which is also an important component for fruit yield. The two FW QTL (*qfw2.1*, *qfw3.2*) are co-localized with consensus FSI QTL (*qfsi2.2*, *qfsi3.1*, respectively indicating a close correlation between them (Table 4; Fig. S5). In published studies of fruit size/shape traits, the major QTL for FL and FW in cucumber were co-localized on the same chromosome [50], which was similar to our results. Almost all FW QTL are co-localized with consensus FS QTL indicating a close correlation between them in cucumber. In addition, we compared the genomic regions underlying the 20 QTL for fruit size and shape from our study with consensus FS and FW QTL inferred by Pan et al. (2020) [50], we found that there are 14 novel QTL (*qfd2.1*, *qfd6.1*, *qfd8.1*, *qfd9.1*, *qfl2.1*, *qfl5.2*, *qfl6.1*, *qfl8.1*, *qfsi2.1*, *qfw3.1*, *qfw3.2*, *qfw6.1*, *qfw8.1*) not identified in previous studies.

QTL for seed size and weight in watermelon

In this study, QTL analysis identified nine QTL for SL, SW and 20-SWT with 4, 3, and 2 for SL, SW, and 20-SWT, respectively (Table 4; Fig. S6). Guo et al. (2020) reviewed the genetic architecture of seed size variation in watermelon, and inferred 14 consensus QTL on seed size and which are distributed on 7 of the 11 watermelon chromosomes [1,17,52-55]. Among them, *qsl5.1*, *qsl5.2*, *qsl7.1*, *qsw3.1*, *qsw10.1*, *q20swt10.1* were not identified in previous studies. Especially, the QTL on chromosome 6, was identified in most studies with F_2 and RILs populations derived from different seed size materials, suggesting that this QTL may play the most important role in seed size/weight determination [17,54,55,76]. Interestingly, we detected a major-effect QTL (PVE = 35.5-50.1%) for SL, SW, and 20SWT (20 seed weight) on chromosome 2 by two watermelon inbred lines with medium size seeds, and we detected none QTL on chromosome 6. Indeed, the major-effect QTL was probably the same one detected in multiple previous studies controlling seed size variation in watermelon [1,17,76]. So the QTL on chromosome 2 may control medium size seed variation in watermelon.

Conclusion

In the present work, we constructed a high-density genetic map in watermelon based on the GBS method. Combined the high-throughput sequencing and strict filtering pipeline, we identified high-quality SNPs in F_2 population and created a high-density genetic map that contained 1004 bin markers evenly distributed across the 11 watermelon chromosomes. The genetic map spanned 1261.1 cM with an average distance of 1.26 cM between adjacent markers, and 47 QTL for fruit and seed-related traits were mapped. The location of these QTL in narrow genomic intervals could facilitate cloning of the underlying genes and their use in breeding programs by marker-assisted selection. Since the mapping population was developed from commercial cultivars, avoiding the negative consequences associated to linkage drag when using exotic material as donors. Results from this study will lay the foundation for further fine mapping, marker-assisted selection and map-based gene cloning in watermelon.

Abbreviations

FW, fruit weight; FFC, fruit flesh color; RC, rind color; RSP, rind stripe pattern; BCC, brix content central; BCE, brix content edge; SL, seed length; SW, seed width; 20SWT, 20-seed weight; FD, fruit diameter; FL, fruit length; FSI, fruit shape index.

Declarations

Ethics approval and consent to participate

The research on watermelon QTL mapping in the manuscript has been conducted under the guidance of international ethical standards. All research protocols were conducted with the approval of the Qiqihar University, China.

Consent to publish

All authors are agree and gave their consent to publish this manuscript.

Availability of data and materials

All data pertinent to this study have been provided in supplemental materials of this manuscript.

Competing interests

There are no known conflicts of interest associated with this publication and there has been no significant financial support for this work that could have influenced its outcome.

Funding

This work was supported by the National Natural Science Foundation of China (31972437 31772334 31401891), the Natural Science Foundation of Heilongjiang Province (LC2018015), and the Fundamental Research Funds of Heilongjiang Provincial Universities (135209106) to MG. Funds were used the design of the study and collection, analysis, and interpretation of data and in writing the manuscript. All the expenses come in conducted the experiment was supported by National Natural Science Foundation of China, the Natural Science Foundation of Heilongjiang Province and the Fundamental Research Funds of Heilongjiang Provincial Universities.

Authors' Contributions

MG conceived the research, designed the experiments. XL performed the research, analyzed the data, and prepared draft of the manuscript. XL, YG, HX, JL, YG, and CY participated in data collection, FL provided theoretical guidance. All authors are agree and gave their consent to publish this manuscript.

Acknowledgements

We thank the college of life sciences, agriculture and forestry, Qiqihar University, China and Qiqihar Horticultural Research Institute, China for the assistance.

References

1. Kim KH, Hwang JH, Han DY, Park M, Kim S, Choi D, et al. Major quantitative trait loci and putative candidate genes for powdery mildew resistance and fruit-related traits revealed by an intraspecific genetic map for watermelon (*Citrullus lanatus lanatus*). PLoS One. 2015;10: e0145665.

2. Elshire RJ, Glaubitz JC, Sun Q, Poland JA, Kawamoto K, Buckler ES, et al. A robust, simple genotyping-by-sequencing (GBS) approach for high diversity species. PLoS One. 2011;6: e19379.
3. DeLeon TB, Linscombe S, Subudhi PK. Molecular dissection of seedling salinity tolerance in rice (*Oryza Sativa*) using a high-density GBS-based SNP linkage map. Rice. 2016;9:52.
4. Li HH, Vikram P, Singh RP, Kilian A, Carling J, Song J, et al. A high density GBS map of bread wheat and its application for dissecting complex disease resistance traits. BMC Genomics. 2015;16:216.
5. Poland JA, Brown PJ, Sorrells ME, Jannink JL, Yin T. Development of high-density genetic maps for barley and wheat using a novel two-enzyme genotyping-by-sequencing approach. PLoS One. 2012;7:e32253.
6. Chen ZL, Wang BB, Dong XM, Liu H, Ren LH, Chen J, et al. An ultra-high density bin-map for rapid QTL mapping for tassel and ear architecture in a large F_2 maize population. BMC Genomics. 2014;15:433.
7. Nimmakayala P, Abburi VL, Bhandary A, Abburi L, Vajja VG, Reddy R, et al. Use of VeraCode 384-plex assays for watermelon diversity analysis and integrated genetic map of watermelon with single nucleotide polymorphisms and simple sequence repeats. Mol Breed. 2014;34:537-548.
8. Reddy UK, Nimmakayala P, Levi A, Abburi VL, Saminathan T, Tomason YR, et al. High-resolution genetic map for understanding the effect of genome-wide recombination rate on nucleotide diversity in watermelon. G3. 2014;4:2219-2230.
9. Wu S, Wang X, Reddy U, Sun H, Bao K, Gao L, et al. Genome of 'Charleston Gray', the principal American watermelon cultivar, and genetic characterization of 1,365 accessions in the U.S. National Plant Germplasm System watermelon collection. Plant Biotechnol J. 2019;17:2246-2258.
10. Ren RS, Ray R, Li PF, Xu JH, Zhang M, Liu G, et al. Construction of a high density DArTseq SNP-based genetic map and identification of genomic regions with segregation distortion in a genetic population derived from a cross between feral and cultivated-type watermelon. Mol Genet Genomics. 2015;290:1457.
11. Shang JL, Li N, Li NN, Xu Y, Ma SW, Wang JM. Construction of a high-density genetic map for watermelon (*Citrullus lanatus*) based on large-scale SNP discovery by specific length amplified fragment sequencing (SALF-seq). Sci Hortic-Amsterdam. 2016;203:38-46.
12. Branham S, Vexler L, Meir A, Tzuri G, Frieman Z, Levi A, et al. Genetic mapping of a major codominant QTL associated with β-carotene accumulation in watermelon. Mol Breed. 2017;37:146.
13. Li BB, Lu XQ, Dou JL, Aslam A, Gao L, Zhao SJ, et al. Construction of a high-density genetic map and mapping of fruit traits in watermelon (*Citrullus Lanatus*) based on whole-genome resequencing. Int J Mol Sci. 2018;19:3268.
14. Guner N, Wehner TC. The genes of watermelon. Hortscience. 2004;39:1175-1182.
15. Sandlin K, Prothro J, Heesacker A, Khalilian N, Okashah R, Xiang W, et al. Comparative mapping in watermelon [*Citrullus lanatus* (thunb.) Matsum et Nakai]. Theor Appl Genet. 2012;125:1603-1618.

16. Ren Y, Zhao H, Kou Q, Jiang J, Guo S, Zhang H, et al. A high resolution genetic map anchoring scaffolds of the sequenced watermelon genome. PLoS One. 2012;7:e29453.
17. Ren Y, McGregor C, Zhang Y, Gong G, Zhang H, Guo S, et al. An integrated genetic map based on four mapping populations and quantitative trait loci associated with economically important traits in watermelon (*Citrullus lanatus*). BMC Plant Biol. 2014;14:33.
18. Zhu HY, Song PY, Koo DH, Guo LQ, Li YM, Sun SR, et al. Genome wide characterization of simple sequence repeats in watermelon genome and their application in comparative mapping and genetic diversity analysis. BMC Genomics. 2016;17(1):557.
19. Guo SG, Zhao SJ, Sun HH, Wang X, Wu S, Lin T, et al. Resequencing of 414 cultivated and wild watermelon accessions identifies selection for fruit quality traits. Nat Genet. 2019;51:1616-1623.
20. Gusmini G, Wehner TC. Qualitative inheritance of rind pattern and flesh color in watermelon. J Hered. 2006;97:177-185.
21. Kumar R, Wehner TC. Discovery of second gene for solid dark green versus light green rind pattern in watermelon. J Hered. 2011;102:489-493.
22. Park SW, Kim KT, Kang SC, Yang HB. Rapid and practical molecular marker development for rind traits in watermelon. Hortic Environ Biote. 2016;57:385-391.
23. Dou JL, Lu XQ, Ali A, Zhao SJ, Zhang L, He N, et al. Genetic mapping reveals a marker for yellow skin in watermelon (*Citrullus lanatus*). PLoS One. 2018;13:e0200617.
24. Liu D, Yang H, Yuan Y, Zhu H, Zhang M, Wei X, et al. Comparative transcriptome analysis provides insights into yellow rind formation and preliminary mapping of the *Clyr* (yellow rind) gene in watermelon. Front Plant Sci. 2020;11:192.
25. Li BB, Zhao SJ, Dou JL, Aslam A, Gebremeskel H, Gao L, et al. Genetic mapping and development of molecular markers for a candidate gene locus controlling rind color in watermelon. Theor Appl Genet. 2019;132:2741-2753.
26. Weetman LM. Inheritance and correlation of shape, size, and color in the watermelon, *Citrullus vulgaris* Iowa Agr Expt Sta Res Bul. 1937;228:342-350.
27. Poole CF. Genetics of cultivated cucurbits. J Hered. 1944;35:122-128.
28. Rhodes BB. Genes affecting foliage color in watermelon. J Hered. 1986;77:134-135.
29. Yang HB, Park S, Park Y, Lee GP, Kang SC, Kim YK. Linkage analysis of the three loci determining rind color and stripe pattern in watermelon. Kor J Hort Sci Technol. 2015;33:559-565.
30. Lou LL, Wehner TC. Qualitative inheritance of external fruit traits in watermelon. Hortscience. 2016;51:487-496.
31. Gama RN, Santos CA, Dias RC, Alves JC, Nogueira TO. Microsatellite markers linked to the locus of the watermelon fruit stripe pattern. Genet Mol Res. 2015;14:269-276.
32. Kim H, Han D, Kang J, Choi Y, Levi A, Lee GP, et al. Sequence-characterized amplified polymorphism markers for selecting rind stripe pattern in watermelon (*Citrullus lanatus*). Hortic Environ Biote. 2015;56:341-349.

33. Zhang ZP, Zhang YN, Sun L, Qiu G, Sun YJ, Zhu ZC, et al. Construction of a genetic map for, *Citrullus lanatus*, based on CAPS markers and mapping of three qualitative traits. Sci Hortic-Amsterdam. 2018;233:532-538.
34. Perkins-Veazie P, Collins JK, Davis AR, Roberts W. Carotenoid content of 50 watermelon cultivars. J Agr Food Chem. 2006;54:2593-2597.
35. Bang H, Davis AR, Kim S, Leskovar DI, King SR. Flesh color inheritance and gene interactions among canary yellow, pale yellow, and red watermelon. J Am Soc Hortic Sci. 2010;135:362-368.
36. Wang C, Qiao A, Fang X, Sun L, Gao P, Davis AR, et al. Fine mapping of lycopene content and flesh color related gene and development of molecular marker–assisted selection for flesh color in watermelon (*Citrullus lanatus*). Front Plant Sci. 2019;10:1240.
37. Bang H, Kim S, Leskovar D, King S. Development of a codominant CAPS marker for allelic selection between canary yellow and red watermelon based on SNP in l*ycopene β-cyclase* (*LCYB*) gene. Mol Breed. 2007;20:63-72.
38. Liu S, Gao P, Wang XZ, Davis AR, Baloch AM, Luan FS. Mapping of quantitative trait loci for lycopene content and fruit traits in *Citrullus lanatus*. Euphytica. 2015;202:411-426.
39. Nakkanong K, Yang JH, Zhang MF. Carotenoid accumulation and carotenogenic gene expression during fruit development in novel interspecific inbred squash lines and their parents. J Agr Food Chema. 2012;60:5936-5944.
40. Grassi S, Piro G, Lee JM, Zheng Y, Fei ZJ, Dalessandro G, et al. Comparative genomics reveals candidate carotenoid pathway regulators of ripening watermelon fruit. BMC Genomics. 2013;14:781.
41. Lv P, Li N, Liu H, Gu HH, Zhao WE. Changes in carotenoid profiles and in the expression pattern of the genes in carotenoid metabolisms during fruit development and ripening in four watermelon cultivars. Food Chem. 2015;174:52-59.
42. Guo S, Sun H, Zhang H, Liu J, Ren Y, Gong G, et al. Comparative transcriptome analysis of cultivated and wild watermelon during fruit development. PLoS One. 2015;10:e0130267.
43. Ren Y, Guo S, Zhang J, He H, Sun H, Tian S, et al. A tonoplast sugar transporter underlies a sugar accumulation QTL in watermelon. Plant Physiol. 2018;176:836-850.
44. McKay JW. Factor interaction in Citrullus. J Hered. 1936;27:110-112.
45. Poole CF, Grimball PC. Interaction of sex, shape, and weight genes in watermelon. J Agric Res. 1945;71:533-552.
46. Tanaka T, Wimol S, Mizutani T. Inheritance of fruit shape and seed size of watermelon. J Jpn Soc Hortic Sci. 1995;64:543-548.
47. Gusmini G, Wehner TC. Foundations of yield improvement in watermelon. Crop Sci. 2005;45:141-146.
48. Gusmini G, Wehner TC. Heritability and genetic variance estimates for fruit weight in watermelon. Hortscience. 2007;42:1332-1336.
49. Kumar R, Wehner TC. Quantitative analysis of generations for inheritance of fruit yield in watermelon. Hortscience. 2013;48:844-847.

50. Pan YP, Wang YH, McGregor C, Liu S, Luan FS, Gao ML, et al. Genetic architecture of fruit size and shape variation in cucurbits: a comparative perspective. Theor Appl Genet. 2020;133:1-21.
51. Yongjae K, Taejin Y, Younghoon P, Yongjik L, Suncheol K, Yongkwon K, et al. Development of near isogenic lines with various seed sizes and study on seed size-related characteristics in watermelon. Korean J Breed Sci. 2009;41:403-411.
52. Guo Y, Gao M, Liang X, Xu M, Liu X, Zhang Y, et al. Quantitative trait loci for seed size variation in cucurbits - A review. Front Plant Sci. 2020;11:304.
53. Meru G, McGregor C. Genetic mapping of seed traits correlated with seed oil percentage in watermelon. Hortscience. 2013;48:955-959.
54. Liu CQ, Gao P, Luan FS. Construction of a genetic linkage map and QTL analysis of fruit-associated traits in watermelon. Sci Agric Sin. 2014;47:2814-2829.
55. Li N, Shang JL, Wang JM, Zhou D, Li NN, Ma SW. Fine mapping and discovery of candidate genes for seed size in watermelon by genome survey sequencing. Sci Rep. 2018;8:843-854.
56. Pereira L, Ruggieri V, Pérez S, Alexiou KG, Fernández M, Jahrmann T, et al. QTL mapping of melon fruit quality traits using a high-density GBS-based genetic map. BMC Plant Biol. 2018;18:324.
57. Gao ML, Hu LL, Li YH, Weng YQ. The chlorophyll-deficient golden leaf mutation in cucumber is due to a single nucleotide substitution in *CsChlI* for magnesium chelatase I subunit. Theor Appl Genet. 2016;129:1961-1973.
58. Guo S, Zhang J, Sun H, Salse J, Lucas WJ, Zhang H, et al. The draft genome of watermelon (*Citrullus lanatus*) and resequencing of 20 diverse accessions. Nat Genet. 2013;45:51-58.
59. Li H, Durbin R. Fast and accurate short read alignment with burrows-wheeler transform. Bioinformatics. 2009;25:1754-1760.
60. Koboldt DC, Zhang QY, Larson DE, Shen D, Mclellan MD, Lin L, et al. VarScan 2: somatic mutation and copy number alteration discovery in cancer by exome sequencing. Genome Res. 2012;22:568-576.
61. DePristo MA, Banks E, Poplin R, Garimella KV, Maguire JR, Hartl C, et al. A framework for variation discovery and genotyping using next-generation DNA sequencing data. Nat Genet. 2011;43:491-498.
62. Wang K, Li MY, Hakonarson H. ANNOVAR: functional annotation of genetic variants from high-throughput sequencing data. Nucleic Acids Res. 2010;38:e164-e164.
63. Broman KW, Wu H, Sen S, Churchill GA. R/qtl: QTL mapping in experimental crosses. Bioinformatics. 2003;19:889-890.
64. Weng Y, Colle M, Wang Y, Yang L, Rubinstein M, Sherman A, et al. QTL mapping in multiple populations and development stages reveals dynamic QTL for fruit size in cucumbers of different market classes. Theor Appl Genet. 2015;128:1747-1763.
65. Churchill GA, Doerge RW. Empirical threshold values for quantitative trait mapping. Genetics. 1994;138:963-971.

66. Doerge RW, Churchill GA. Permutation tests for multiple loci affecting a quantitative character. Genetics. 1996;142:285-294.
67. Bo KL, Ma Z, Chen JF, Weng YQ. Molecular mapping reveals structural rearrangements and quantitative trait loci underlying traits with local adaptation in semi-wild Xishuangbanna cucumber (*Cucumis sativus* var. *xishuangbannanesis* Qi et Yuan). Theor Appl Genet. 2015;128,25-39.
68. Hashizume T, Shimamoto I, Harushima Y, Yui M, Sato T, Imai T, et al. Construction of a linkage map for watermelon (*Citrullus lanatus* (Thunb.) Matsum & Nakai) using random amplified polymorphic DNA (RAPD). Euphytica. 1996;90(3):265-273.
69. Levi A, Thomas CE, Zhang X, Joobeur T, Dean RA, Wehner TC, et al. A genetic linkage map for watermelon based on randomly amplifed polymorphic DNA markers. J Am Soc Hortic Sci. 2001;126:730-737.
70. Levi A, Thomas C, Trebitsh T, Salman A, King J, Karalius J, et al. An extended linkage map for watermelon based on SRAP, AFLP, SSR, ISSR, and RAPD markers. J Am Soc Hortic Sci. 2006;131(3):393-402.
71. Zhang Q, Liu CY, Liu YF, VanBuren R, Yao XH, Zhong CH, et al. High-density interspecific genetic maps of kiwifruit and the identification of sex-specific markers. DNA Res. 2015;22:367-375.
72. Wehner TC. Gene list for watermelon. Cucurbit Genet Coop Rep (2007) 30: 96-120
73. Henderson WR, Scott GH, Wehner TC. Interaction of flesh color genes in watermelon. J Hered. 1998;89:50-53.
74. Dou JL, Zhao SJ, Lu XQ, He N, Zhang L, Ali Aslam, et al. Genetic mapping reveals a candidate gene (*ClFS1*) for fruit shape in watermelon (*Citrullus lanatus*). Theor Appl Genet. 2018;131:947-958.
75. Maragal S, Rao ES, Lakshmana Reddy DC. Genetic analysis of fruit quality traits in prebred lines of watermelon derived from a wild accession of *Citrullus amarus*. Euphytica. 2019;215:199.
76. Legendre R, Kuzy J, Mcgregor C. Markers for selection of three alleles of *ClSun25-26-27a* (c*la011257*) associated with fruit shape in watermelon. Mol Breed. 2020;40:19.
77. Prothro J, Sandlin K, Abdel-Haleem H, Bachlava E, Mcgregor C. Main and epistatic quantitative trait loci associated with seed size in watermelon. J Am Soc Hortic Sci. 2012;137:452-457.

Tables

Due to technical limitations, table 1, table 2, table 3 and table 4 are available as a download in the Supplemental Files section.

Figures

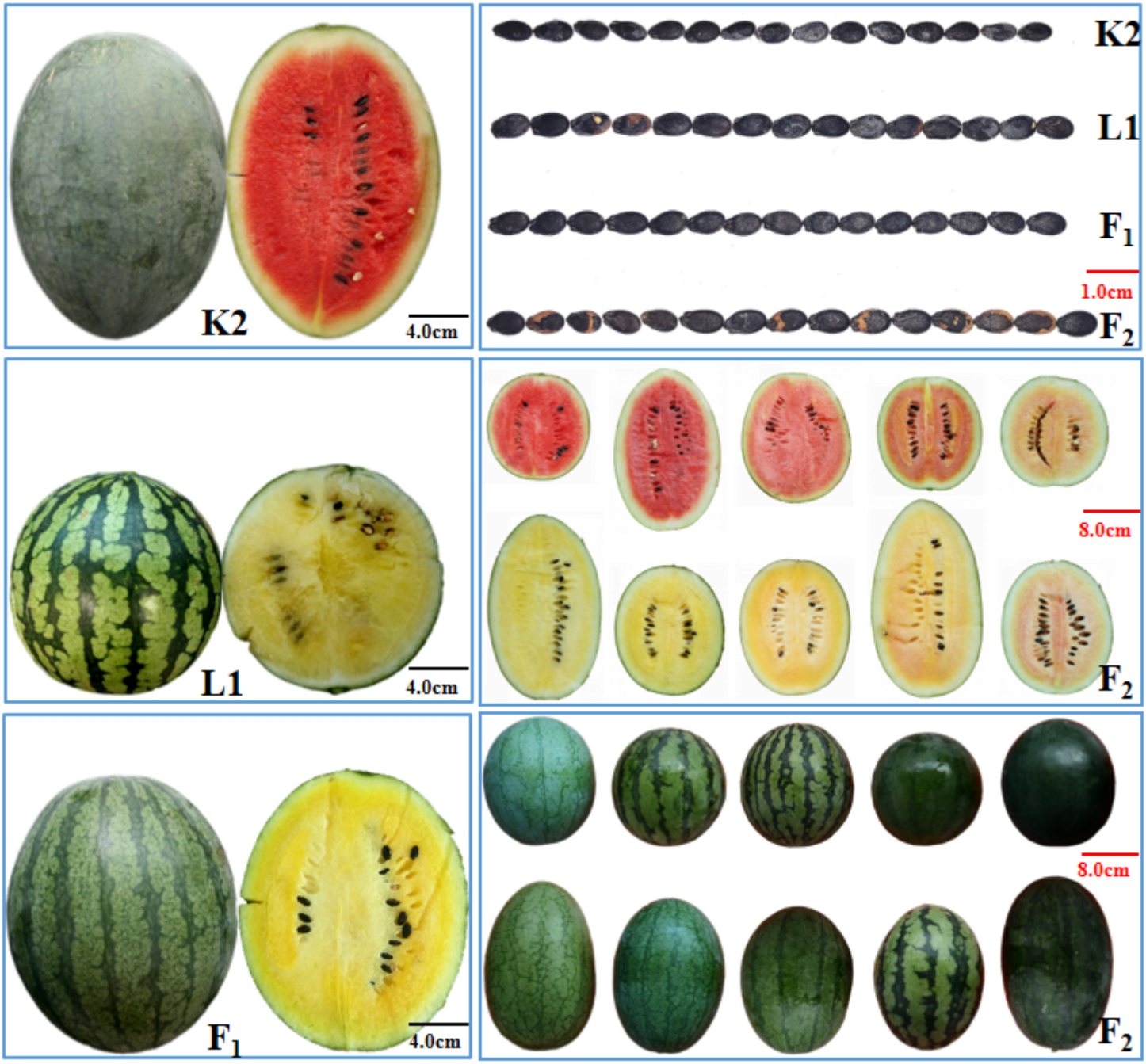

Figure 1

Morphological differences of two parental lines used in the present study. Fruits of K2 are oval shaped with smooth, dark green rind, and red flesh; Fruits of L1 are round with striped rind and yellow flesh. The seeds of K2 are uniformly dark, and those from L1 are stippled but slightly larger.

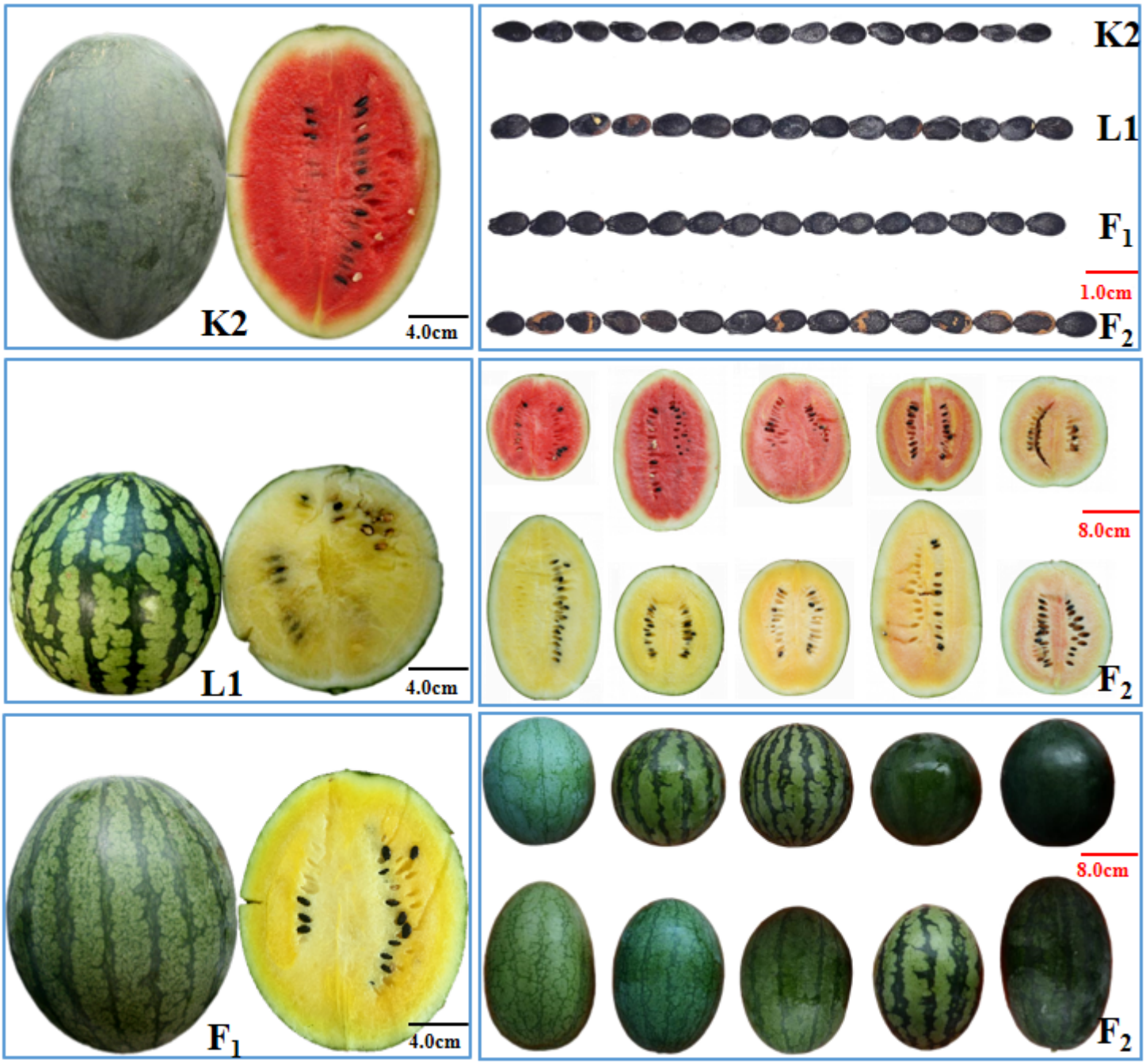

Figure 1

Morphological differences of two parental lines used in the present study. Fruits of K2 are oval shaped with smooth, dark green rind, and red flesh; Fruits of L1 are round with striped rind and yellow flesh. The seeds of K2 are uniformly dark, and those from L1 are stippled but slightly larger.

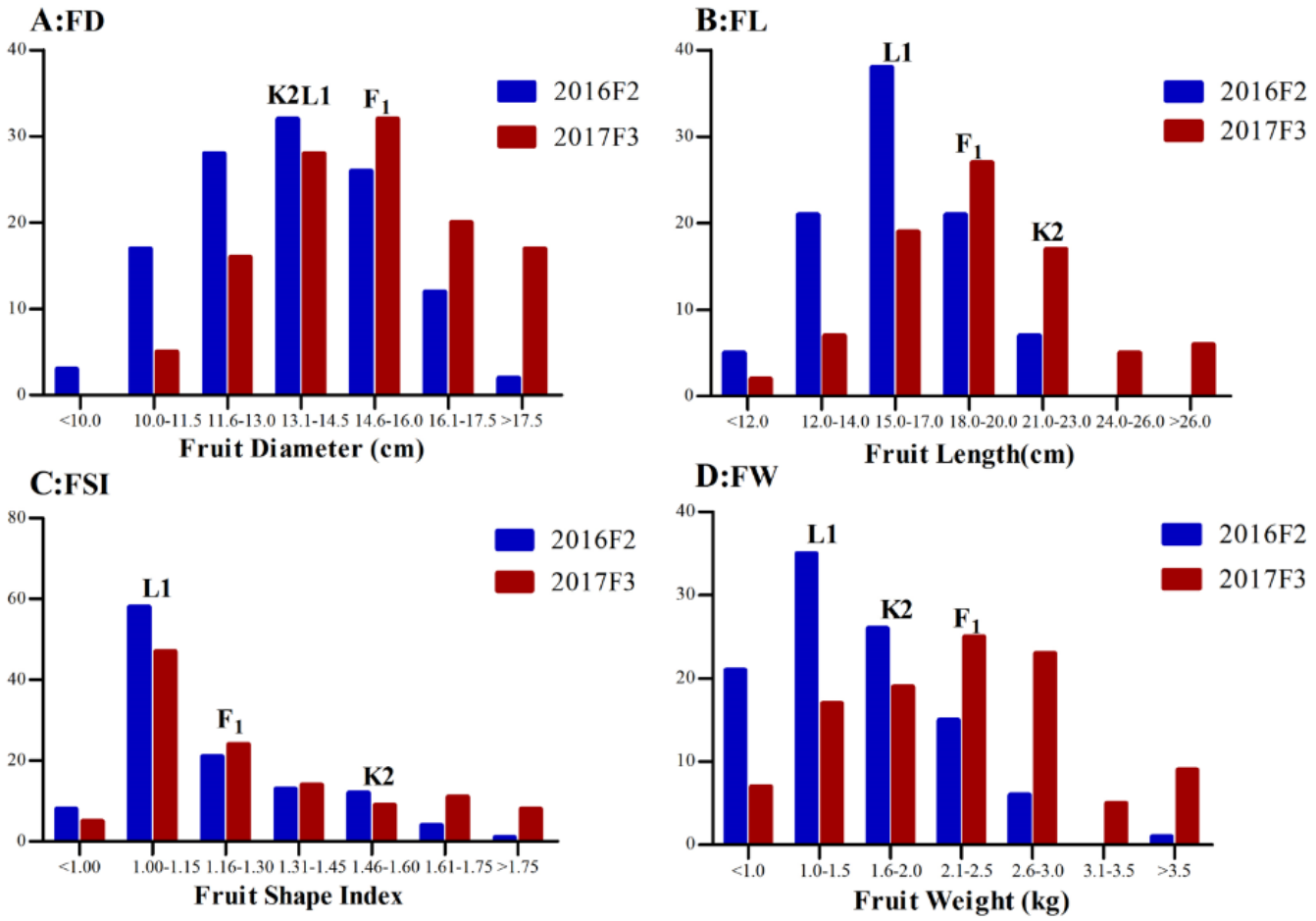

Figure 2

Frequency distribution of rind color (RC), rind stripe pattern (RSP), flesh color (FFC), fruit weight (FW), fruit diameter (FD), fruit length (FL) and fruit shape index (FSI) among 120 K2× L1 F2:3 families in two experiments (2016F2 and 2017F3). Arrows indicated corresponding values of K2, L1 and their F1.

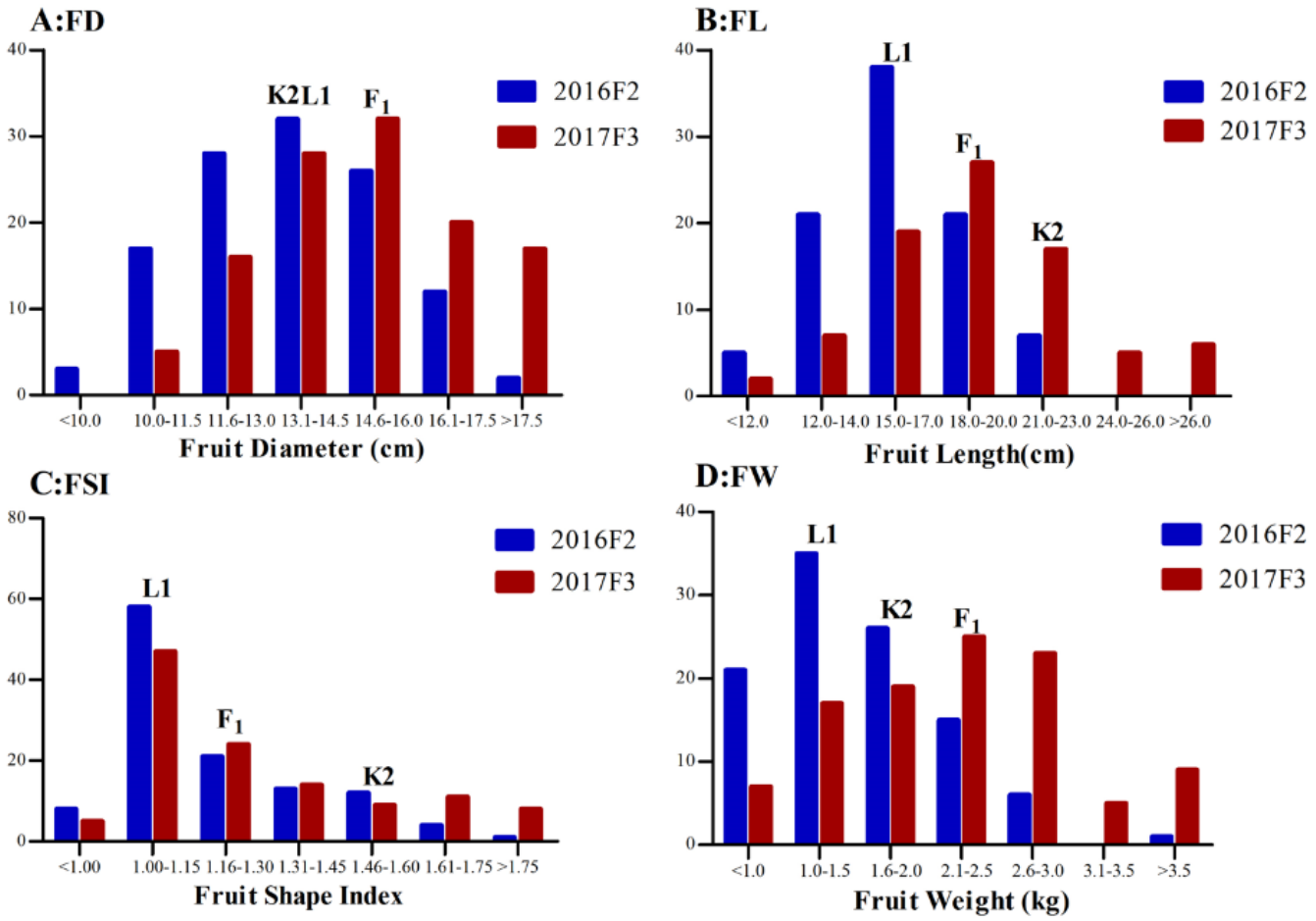

Figure 2

Frequency distribution of rind color (RC), rind stripe pattern (RSP), flesh color (FFC), fruit weight (FW), fruit diameter (FD), fruit length (FL) and fruit shape index (FSI) among 120 K2× L1 F2:3 families in two experiments (2016F2 and 2017F3). Arrows indicated corresponding values of K2, L1 and their F1.

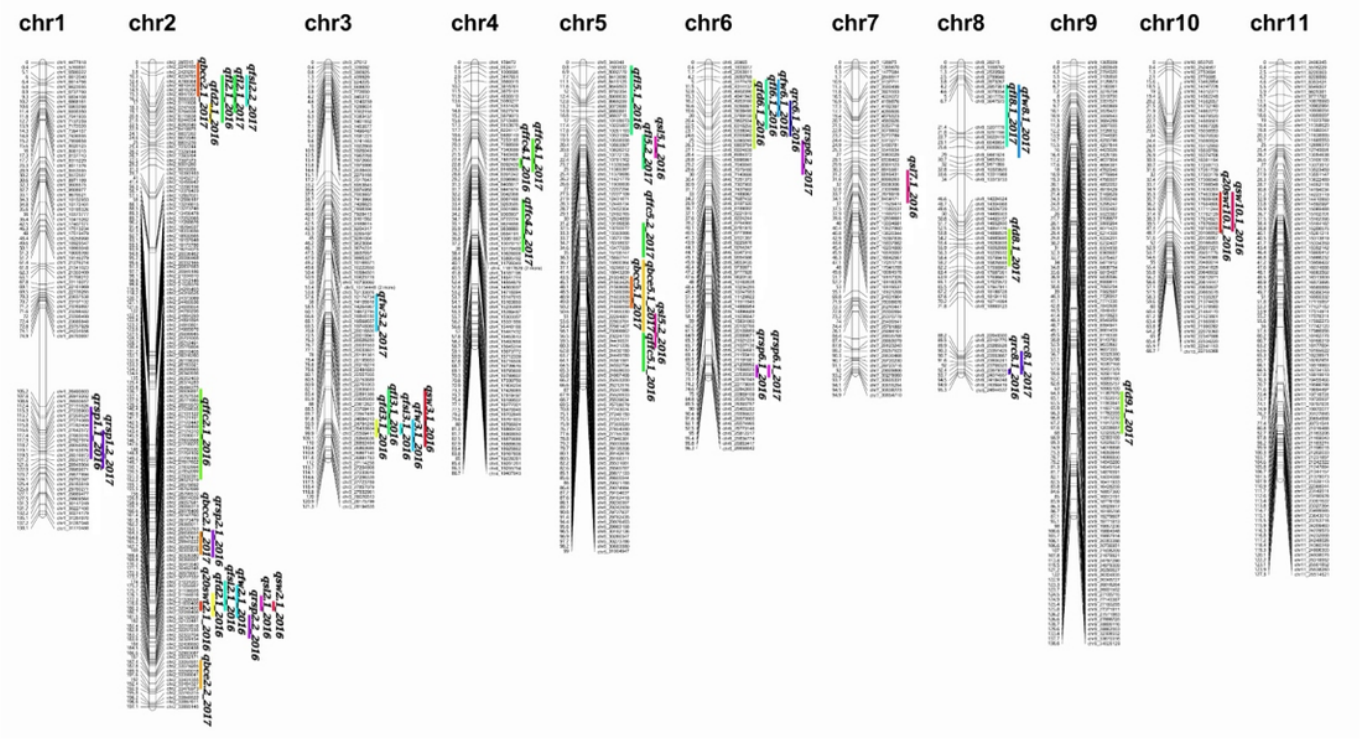

Figure 3

Genetic map containing detected QTL and major loci. The map distance is given on the left in cM from the top of each chromosome. Vertical bars delimit positions of QTL in terms of 1.5-LOD interval. FW, fruit weight; FFC, fruit flesh color; RC, rind color; RSP, rind stripe pattern; BCC, brix content central; BCE, brix content edge; SL, seed length; SW, seed width; 20SWT, 20-seed weight; FD, fruit diameter; FL, fruit length; FSI, fruit shape index.

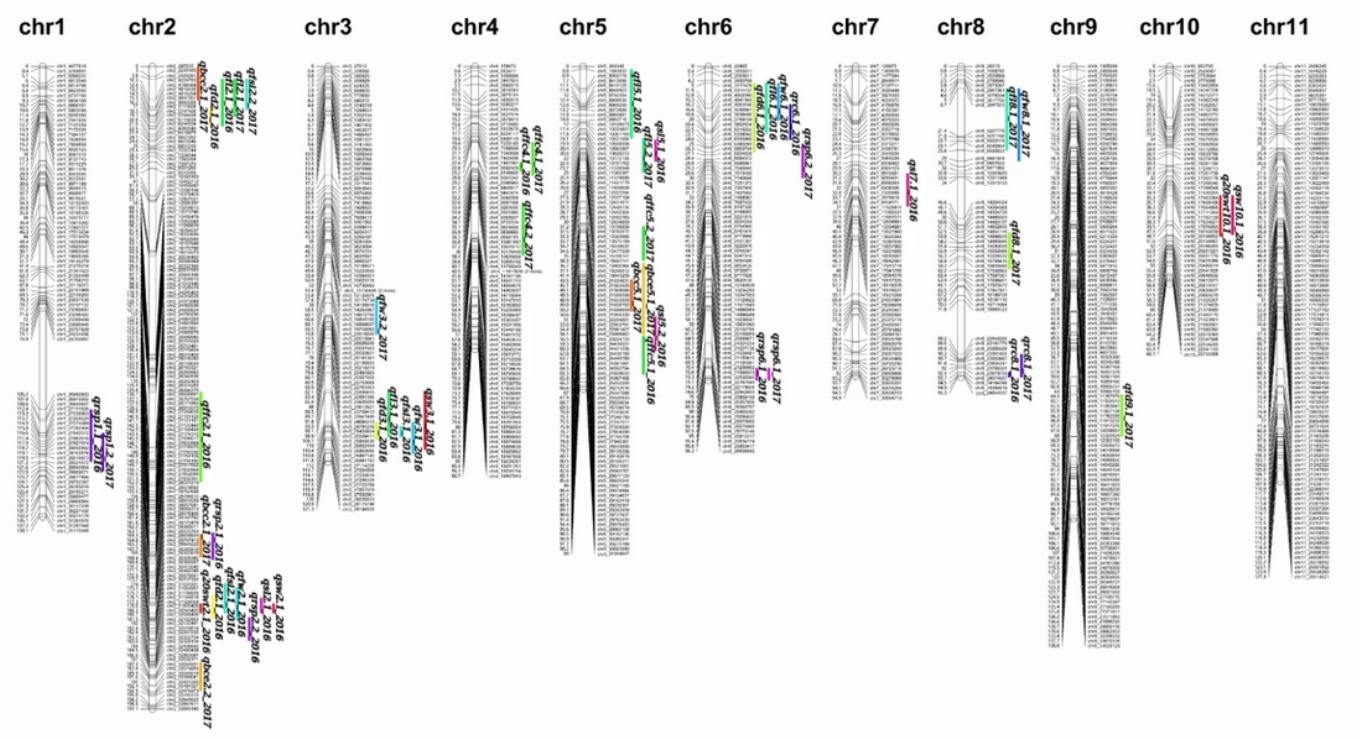

Figure 3

Genetic map containing detected QTL and major loci. The map distance is given on the left in cM from the top of each chromosome. Vertical bars delimit positions of QTL in terms of 1.5-LOD interval. FW, fruit weight; FFC, fruit flesh color; RC, rind color; RSP, rind stripe pattern; BCC, brix content central; BCE, brix content edge; SL, seed length; SW, seed width; 20SWT, 20-seed weight; FD, fruit diameter; FL, fruit length; FSI, fruit shape index.

Supplementary Files

This is a list of supplementary files associated with this preprint. Click to download.

- SupplTablesS1S3.xlsx
- SupplTablesS1S3.xlsx
- SuppFig.S1S6.pptx
- SuppFig.S1S6.pptx
- Tables14.xlsx
- Tables14.xlsx